



Two-photon excited photoluminescence of single perovskite nanocrystals

Cite as: J. Chem. Phys. **151**, 154201 (2019); <https://doi.org/10.1063/1.5124734>

Submitted: 16 August 2019 . Accepted: 25 September 2019 . Published Online: 15 October 2019

Zengle Cao, Bihu Lv, Huichao Zhang, Yan Lv, Chunfeng Zhang , Yong Zhou, Xiaoyong Wang , and Min Xiao

COLLECTIONS

Paper published as part of the special topic on [Colloidal Quantum Dots](#)

Note: This paper is part of the JCP Special Topic on Colloidal Quantum Dots.

 This paper was selected as Featured



View Online



Export Citation



CrossMark

ARTICLES YOU MAY BE INTERESTED IN

[On the determination of absorption cross section of colloidal lead halide perovskite quantum dots](#)

The Journal of Chemical Physics **151**, 154706 (2019); <https://doi.org/10.1063/1.5126039>

[Trion dynamics in lead halide perovskite nanocrystals](#)

The Journal of Chemical Physics **151**, 170902 (2019); <https://doi.org/10.1063/1.5125628>

[Size and temperature dependence of photoluminescence of hybrid perovskite nanocrystals](#)

The Journal of Chemical Physics **151**, 154705 (2019); <https://doi.org/10.1063/1.5124025>

Lock-in Amplifiers
up to 600 MHz



Zurich
Instruments



Two-photon excited photoluminescence of single perovskite nanocrystals



Cite as: J. Chem. Phys. 151, 154201 (2019); doi: 10.1063/1.5124734

Submitted: 16 August 2019 • Accepted: 25 September 2019 •

Published Online: 15 October 2019



View Online



Export Citation



CrossMark

Zengle Cao,¹ Bihu Lv,² Huichao Zhang,³ Yan Lv,¹ Chunfeng Zhang,¹ Yong Zhou,¹ Xiaoyong Wang,^{1,a)} and Min Xiao^{1,4}

AFFILIATIONS

¹National Laboratory of Solid State Microstructures, School of Physics, and Collaborative Innovation Center of Advanced Microstructures, Nanjing University, Nanjing 210093, China

²Research Center for Smart Sensing, Zhejiang Lab, Hangzhou 311121, China

³College of Electronics and Information, Hangzhou Dianzi University, Xiasha Campus, Hangzhou 310018, China

⁴Department of Physics, University of Arkansas, Fayetteville, Arkansas 72701, USA

Note: This paper is part of the JCP Special Topic on Colloidal Quantum Dots.

^{a)}Electronic mail: wxiaoyong@nju.edu.cn

ABSTRACT

Lead-halide perovskite nanocrystals (NCs) have emerged as a novel type of semiconductor nanostructure, attracting great research interests in both fundamental science and practical applications. Here, we compare the optical properties of single CsPbI₃ NCs under both one-photon and two-photon excitations, mainly including the photoluminescence (PL) blinking and PL decay dynamics. By means of the PL saturation effect caused by multi-exciton Auger recombination, we have also estimated a two-photon absorption cross section of $\sim 6.8 \times 10^6$ GM for single CsPbI₃ NCs. The ability to realize efficient two-photon excitation of single perovskite NCs with strongly suppressed background fluorescence will help not only to promote their bio-imaging and biolabeling applications but also to reveal and manipulate their delicate electronic structures for potential usage in quantum information processing.

Published under license by AIP Publishing. <https://doi.org/10.1063/1.5124734>

INTRODUCTION

Two-photon excited fluorescence of semiconductor colloidal nanocrystals (NCs) has attracted great research interests in both bio-imaging and biolabeling applications,¹ owing to its higher spatial resolution, deeper penetration depth, and smaller sample damage than those of the one-photon excitation scheme.^{2,3} Being more robust against the photobleaching effect and possessing a larger absorption cross section of $\sim 10^3$ – 10^4 GM (1 GM = 10^{-50} cm⁴ s/photon),^{2,4} semiconductor colloidal NCs of metal-chalcogenides are now treated as a competitive alternative to traditional two-photon excited fluorescent material of organic dye molecules.⁵ Meanwhile, the optical transitions induced by two-photon excitation in semiconductor colloidal NCs have also been actively utilized to achieve up-converted amplified spontaneous emission and lasing,^{6,7} as well as to reveal the symmetry selection rules of excited-state excitons.⁸ In contrast to the intensive research efforts devoted to

ensemble semiconductor colloidal NCs, the relevant single-particle studies are rather limited,^{8–10} although they can potentially provide a more in-depth understanding of the two-photon excitation processes.

Owing to the superior optical and material properties, the bulk films of lead-halide perovskites are now being widely investigated for a variety of optoelectronic applications such as in solar cells,¹¹ light-emitting diodes,^{12,13} photodetectors,¹⁴ and lasers.¹⁵ In the year of 2015, their low-dimensional counterparts of semiconductor colloidal NCs were successfully synthesized with size-dependent energy bandgaps that are dictated by the quantum confinement effect.^{16,17} These perovskite NCs have since been subjected to single-particle optical characterizations, yielding a rich spectrum of necessary information on the fluorescent blinking effect,¹⁸ the single-photon emitting characteristics,^{19–22} and the fine energy-level structures of band-edge excitons.^{23–25} With the subsequent demonstration of quantum interference in the

exciton wave functions,²⁶ single perovskite NCs have stepped into the quantum-information-processing regime, where two-photon excitation can serve as a potent tool to resonantly manipulate the cascaded photons emitted by the biexciton and single exciton.²⁷ Although two-photon or even multiphoton excitations of ensemble perovskite NCs have already been documented in several recent reports,^{28–32} the ability to make similar achievements at the single-particle level is yet to be demonstrated so that novel practical applications beyond the ensemble level could be envisioned and fulfilled.

Here, we synthesize lead-halide perovskite NCs of CsPbI₃ with a photoluminescence (PL) peak of 670 nm at room temperature and measure their single-particle optical properties at two excitation laser wavelengths of 405 and 800 nm, respectively. For the same single CsPbI₃ NC, the 405 nm one-photon and 800 nm two-photon excitations yield quite similar PL blinking and PL decay characteristics. This renders two-photon excitation a convenient tool for routine optical characterizations of single perovskite NCs, with the advantages of increasing the spatial imaging resolution and suppressing the background fluorescence. The ability to realize efficient two-photon excitation of single CsPbI₃ NCs is benefited from their large absorption cross section of $\sim 6.8 \times 10^6$ GM, which poses an enhancement of at least two orders of magnitude over those of traditional metal-chalcogenide NCs. For the estimation of two-photon absorption (TPA) cross section of single CsPbI₃ NCs, we have developed a new approach based on the PL saturation effect caused by multi-exciton Auger recombination, which can be extended to other semiconductor colloidal NCs at both single-particle and ensemble levels.

EXPERIMENTAL

The perovskite CsPbI₃ NCs used in the current experiment were chemically synthesized according to the standard procedures reported previously.^{20,24} In brief, the Cs-oleate precursor was prepared first by loading the mixture of Cs₂CO₃, oleic acid (OA), and octadecene (ODE) into a 100 ml 3-neck flask. The resulted solution was dried under vacuum for 1 h at 120 °C, after which the temperature was elevated to 150 °C and then kept at a stable value of 100 °C. For the synthesis of CsPbI₃ NCs, the PbI₂ and ODE mixture was first loaded into a 50 ml 3-neck flask and then dried under vacuum for 1 h at 120 °C. After quick injection of OA and oleylamine (OLA) under N₂, the solution temperature was elevated to 160 °C for the reaction with the Cs-oleate precursor. The obtained product was kept at this temperature for 5 s and then cooled down to room temperature.

Finally, the CsPbI₃ NCs were purified by high-speed centrifugation (10 000 rpm) for 10 min and then redispersed in toluene to form a stable solution.

One drop of the diluted solution of CsPbI₃ NCs was spin-coated onto a fused silica substrate, which was then placed in a confocal scanning optical microscope for the single-particle optical measurements at room temperature. A 405 nm diode laser with a repetition rate of 5 MHz and a pulse width of ~ 100 ps was used as the one-photon excitation source, while a ~ 4 ps Ti:sapphire laser operated at 800 nm with a repetition rate of either 4.875 or 2 MHz was employed for the two-photon excitation. The laser beam was focused on the sample substrate by an immersion-oil objective with a numerical aperture of 1.4, which was also used to collect the optical signal emitted by a single CsPbI₃ NC. The optical signal could be sent to either a charge-coupled-device camera for the PL spectral measurement with an integration time of 1 s, or two avalanche photodiodes for the PL blinking time trace, single-photon emission and PL decay measurements. To avoid exciting multiple excitons in a single CsPbI₃ NC, the 405 and 800 nm lasers were set at low power densities of ~ 0.3 and 50 W/cm², respectively, unless otherwise specified in the text for the laser-power-density dependent measurements.

RESULTS

Structural and optical properties of ensemble CsPbI₃ NCs

As shown in Fig. 1(a), the as-synthesized CsPbI₃ NCs have a cubic shape with an average edge length of ~ 13.5 nm, which is close to the exciton Bohr diameter of this semiconductor material.¹⁷ The absorption spectrum measured in solution for ensemble CsPbI₃ NCs is plotted in Fig. 1(b), where the lowest-energy band-edge peak is located at ~ 1.93 eV (~ 642.5 nm). The solution PL spectrum of ensemble CsPbI₃ NCs excited at 405 nm is also shown in Fig. 1(b), with a peak energy of ~ 1.85 eV (~ 670.3 nm) that is ~ 110 meV higher than the bulk value of ~ 1.74 eV due to the quantum confinement effect.¹⁷ When spin-coated into a solid film on the substrate, the ensemble CsPbI₃ NCs possess identical PL spectra in Fig. 1(c) under the 405 and 800 nm excitations, with the peak energies being both located at ~ 1.80 eV (~ 687.0 nm). Since the photon energy of 1.55 eV at 800 nm is significantly smaller than 1.80 eV, the PL spectrum obtained at this laser excitation wavelength should truly come from the two-photon excitation.

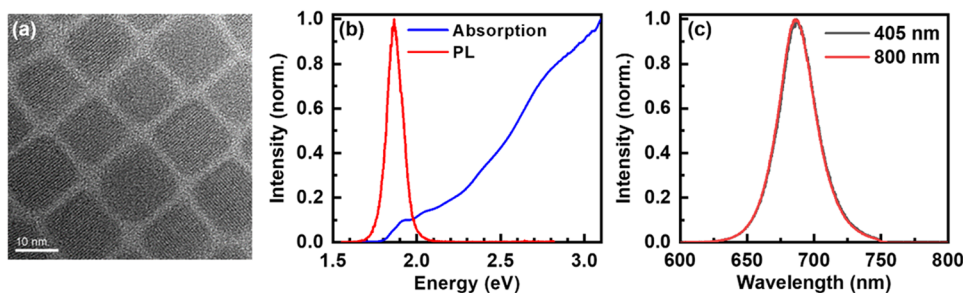


FIG. 1. (a) Transmission electron microscopy image of CsPbI₃ NCs. (b) Solution absorption and PL spectra of CsPbI₃ NCs. (c) PL spectra measured for a solid film of CsPbI₃ NCs at the laser excitation wavelengths of 405 and 800 nm, respectively.

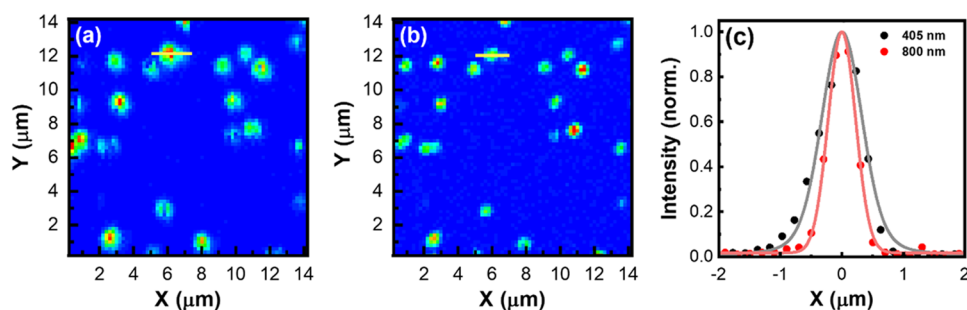


FIG. 2. (a) Confocal scanning PL images of single CsPbI₃ NCs excited at (a) 405 nm and (b) 800 nm, respectively. (c) PL intensity profiles drawn across the solid lines in (a) and (b), and fitted with the Gaussian distributions.

Optical properties of single CsPbI₃ NCs

The confocal scanning PL images obtained with the 405 and 800 nm excitations for the same region of the sample surface are presented in Figs. 2(a) and 2(b), where the single CsPbI₃ NCs are clearly identified with smaller PL spots in the latter case. For a representative CsPbI₃ NC selected from both Figs. 2(a) and 2(b), the PL intensity profiles are drawn along the horizontal direction in Fig. 2(c), and the spatial FWHMs (full-width at half-maximums) of 0.78 and 0.52 μm can be, respectively, extracted by the Gaussian fitting functions. The enhanced spatial resolution achieved with two-photon excitation reflects the fact that, owing to the quadratic dependence on the laser power density, the PL intensity of a single CsPbI₃ NC is very sensitive to its separation distance from the laser spot center.

In the PL spectrum shown in Fig. 3(a) for a single CsPbI₃ NC excited at 800 nm, the PL peak is located at ~ 1.81 eV (~ 685.1 nm) with a FWHM of ~ 90 meV (~ 28.2 nm). Still with the 800 nm excitation, we plot in Fig. 3(b) the second-order photon correlation function measured for a single CsPbI₃ NC, from which a $g^{(2)}(\tau)$ value of ~ 0.1 can be evaluated at $\tau = 0$ to confirm the single-photon emitting feature.²⁰ In Fig. 4, we make side-by-side comparisons between the two complex optical processes of PL blinking and PL decay for the same single CsPbI₃ NC excited at both 405 and 800 nm. As shown, respectively, in Figs. 4(a) and 4(b) for the 405 and 800 nm excitations, the two PL blinking time traces both exhibit long-term “on” periods with the intermittent appearances of short “off” periods whose durations are mostly within the binning time of 100 ms. From statistical measurements on a large number

of single CsPbI₃ NCs, we can safely conclude that no significant difference is observed in the PL blinking properties of a single CsPbI₃ NC with the single-photon and two-photon laser excitations. With the 405 and 800 nm excitations, the two PL decay curves shown in Figs. 4(c) and 4(d) can both be fitted with single-exponential functions, yielding similar PL lifetimes of 81.7 and 91.3 ns, respectively. Based on the above observations, it can be concluded that two-photon excitation can be conveniently employed for the routine optical characterizations of single CsPbI₃ NCs, without suffering from the annoying background fluorescence normally encountered in one-photon excitation especially with high excitation laser energies.

Two-photon absorption cross section of single CsPbI₃ NCs

Due to strong quantum confinement, multiple excitons generated in a single colloidal NC are dissipated mainly through the nonradiative Auger recombination process.²⁰ This would cause the PL saturation effect that can be described by $I \propto 1 - e^{-(N)} = 1 - e^{-\sigma^{(1)}j}$, with I being the PL intensity, j being the laser pump fluence, $\sigma^{(1)}$ being the one-photon absorption cross section, and $\langle N \rangle$ being the average number of excitons created per pulse in a single colloidal NC.^{21,33} From the laser-power-density dependence of the PL intensity measured in Fig. 5(a) for a single CsPbI₃ NC, the one-photon absorption cross section at 405 nm can be extracted to be $\sim 1.9 \times 10^{-14}$ cm², which is consistent with previous values reported for single CsPbBr₃ and CsPbI₃ NCs.^{20,21}

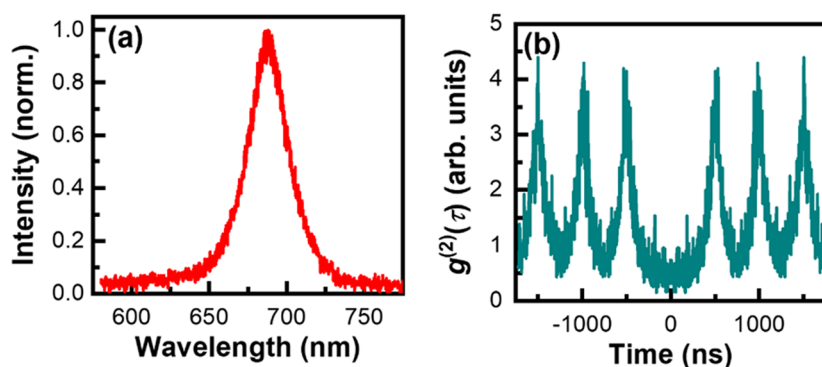


FIG. 3. (a) PL spectrum and (b) second-order photon correlation measurement of single CsPbI₃ NCs excited at 800 nm.

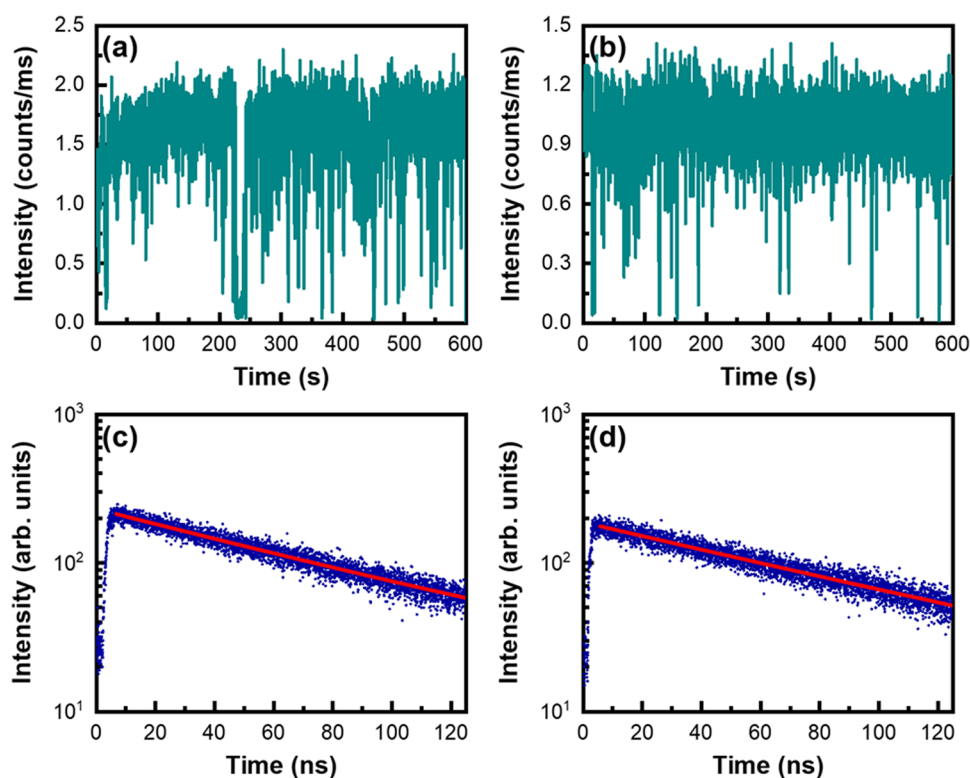


FIG. 4. PL blinking time traces of a single CsPbI₃ NC excited at (a) 405 nm and (b) 800 nm, respectively. PL decay curves of a single CsPbI₃ NC excited at (c) 405 nm and (d) 800 nm and fitted with the single-exponential lifetimes of 81.7 and 91.3 ns, respectively.

So far, several methods have been employed to estimate the two-photon absorption (TPA) cross sections of ensemble perovskite NCs. The first method was originally developed by Xu and Webb to obtain the TPA cross sections for molecular fluorophores by comparison with their one-photon excited fluorescence.⁵ This method requires precise measurements on the quantum yield of fluorescent materials and the collection efficiency of the optical system.^{30,31} In the second method, the Z-scan technique was utilized to estimate the TPA cross sections,^{3,31,34–36} which are based on the non-linear absorption change due to the variation of laser power densities around the focus point. In the third method proposed by Chen *et al.*,²⁸ the TPA cross section was proportional to the linear one-photon absorption, as revealed from the femtosecond transient absorption spectroscopy measurement. Following Xu and Webb's first method, van Oijen *et al.*¹⁰ and Early and Nesbitt⁹ realized the TPA cross section measurements of single CdS and CdSe/ZnS NCs, respectively, while the possible drop of fluorescent quantum efficiency due to the PL blinking effect had to be reasonably corrected. Meanwhile, some reference materials need to be introduced in Xu and Webb's method for the calibration of the fluorescent collection efficiency, which would increase the system complexity and may cause uncontrolled error in determining the TPA cross section.

In analogy to one-photon excitation of single CsPbI₃ NCs discussed earlier in the text, we have worked out a new approach to determine their TPA cross sections by means of the PL saturation

effect ($I \propto 1 - e^{-\langle N \rangle}$) caused by nonradiative Auger recombination of multiple excitons. Under two-photon excitation of a single CsPbI₃ NC, we would have $\langle N \rangle = \frac{g_p}{\tau} \sigma^{(2)} j^2$, where $\sigma^{(2)}$ is the TPA cross section, while τ and $g_p \approx 0.6$ are the width and the time distribution of the excitation laser pulse, respectively.⁵ In Fig. 5(b), we plot the PL intensity measured for a single CsPbI₃ NC as a function of the laser excitation power density. As can be seen in Fig. 5(c), the increase in the NC PL intensity at low laser power densities (<400 W/cm²) can be well fitted by a power-law function with an exponent of ~ 1.94 , thus confirming its two-photon excitation origin. When the laser power density is further increased, the PL intensity shows saturation behavior due to multi-exciton Auger recombination, which can be clearly seen in Fig. 5(d) from its dependence on the square of the laser excitation power density. Using the fitting function of $I \propto 1 - e^{-\langle N \rangle}$ with $\langle N \rangle = \frac{g_p}{\tau} \sigma^{(2)} j^2$, a TPA cross section of $\sigma^{(2)} = 6.7 \times 10^6$ GM can be obtained for this specific CsPbI₃ NC. By statistically measuring ~ 20 single CsPbI₃ NCs in our experiment and plotting the histogram in Fig. 6(a), an average value of $(6.8 \pm 3.1) \times 10^6$ GM can be calculated for $\sigma^{(2)}$, which marks a huge enhancement of at least two orders of magnitude over those of traditional metal-chalcogenide NCs.^{2,4} In contrast to the ensemble measurement that can only yield an average value, the TPA cross sections measured for single CsPbI₃ NCs range from $(1-13) \times 10^6$ GM, which should be a direct consequence of their inhomogeneous size distribution.

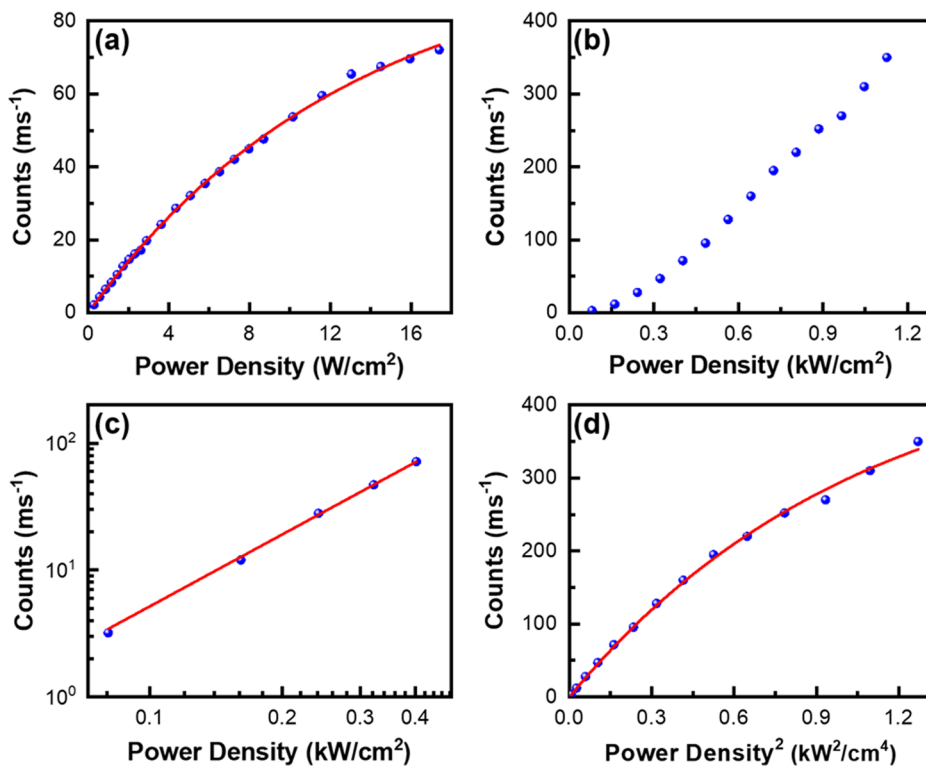


FIG. 5. (a) PL intensity plotted as a function of the laser power density for a single CsPbI₃ NC excited at 405 nm. The data points are fitted by the function form, $\propto 1 - e^{-\sigma^{(1)j}}$, to extract the one-photon absorption cross section (see text). (b) PL intensity plotted as a function of the laser power density for the same single CsPbI₃ NC excited at 800 nm. (c) The data points in (b) are replotted in the log-log scale at low laser-power-density range. The solid line is a power-law fitting with an exponent of ~ 1.94 . (d) The PL intensity data points in (b) are replotted as a function of the square of the laser power density to show the PL saturation effect. The data points are fitted by the function form, $\propto 1 - e^{-\frac{\sigma^2}{T} \sigma^{(2)j^2}}$, to extract the TPA cross section (see text).

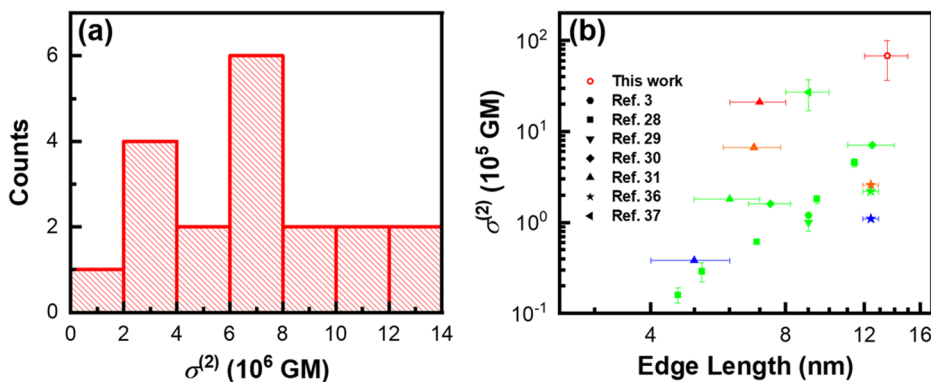


FIG. 6. (a) Statistical histogram showing the distribution of TPA cross sections of ~ 20 single CsPbI₃ NCs. (b) Comparison of TPA cross sections between the literature values and the one obtained in our experiment. The blue, green, and red colors represent CsPbCl₃, CsPbBr₃, and CsPbI₃ NCs, respectively. The TPA cross section values obtained from different references are represented by the data points with different symbols.

DISCUSSIONS

According to previous reports in the literature, the TPA cross sections of semiconductor colloidal NCs are strongly dependent on their sizes and compositions. As revealed by Pu *et al.*, the TPA cross sections were related via the power-law exponents of ~ 3.5 and ~ 5.6 to the diameters of CdSe and CdTe NCs, respectively.³⁷ With the 800 nm excitation on perovskite CsPbBr₃ NCs, Chen *et al.* observed that their TPA cross sections followed the power-law dependence on the edge lengths with an exponent of $\sim 3.3 \pm 0.2$.²⁸ Based on the experimental results from their own and other groups, Nagamine *et al.* suggested that the TPA cross sections of colloidal

metal-chalcogenide and perovskite NCs should be both proportional to their volumes.³⁰ It has also been demonstrated that, for lead-halide perovskite NCs with similar sizes, the TPA cross section should increase sequentially with the changing halide components from Cl to Br, and to I.^{31,35} In Fig. 6(b), we plot the majority of TPA cross section values reported so far by other groups for ensemble perovskite NCs with different edge lengths and compositions,^{3,28–31,35,36} together with the one obtained by us from the single-particle measurement of CsPbI₃ NCs. The TPA cross section of $(6.8 \pm 3.1) \times 10^6$ GM estimated in our current work is relatively larger than all of the other reported values, which is reasonable since our CsPbI₃ NCs are associated with the iodine halide component and

the largest edge length. It should be noted that, while the TPA cross section seems to be fixed once a single perovskite NC has been synthesized, it can be further enhanced by employing external optical structures such as a photonic crystal.³⁸

CONCLUSION

To summarize, we have performed two-photon excitation studies on single perovskite CsPbI₃ NCs at room temperature, which exhibit comparable optical properties to those obtained with one-photon excitation. Based on the PL saturation effect from nonradiative Auger recombination of multiple excitons, we have developed a new method for reliably estimating the TPA cross sections of semiconductor colloidal NCs. The single CsPbI₃ NCs studied here possess an average value of 6.8×10^6 GM for the TPA cross section, which is at least two orders of magnitude higher than those values ever reported for traditional metal-chalcogenide NCs. Such an extremely large TPA cross section implies that low-level laser power density can be routinely used to obtain two-photon excited PL from single perovskite NCs with greatly suppressed background fluorescence. This will not only benefit their practical applications in the traditional areas of biolabeling and bio-imaging but also stimulate their fundamental studies at cryogenic temperatures where resonant manipulations of the exciton wave functions are strongly required.

ACKNOWLEDGMENTS

This work was supported by the National Key R&D Program of China (Grant No. 2017YFA0303700), the National Natural Science Foundation of China (Grant Nos. 61605037, 11574147, and 11621091), and the PAPD of Jiangsu Higher Education Institutions.

REFERENCES

- H. E. Grecco, K. A. Lidke, R. Heintzmann, D. S. Lidke, C. Spagnuolo, O. E. Martinez, E. A. Jares-Erijman, and T. M. Jovin, *Microsc. Res. Tech.* **65**, 169 (2004).
- R. Zhang, E. Rothenberg, G. Fruhwirth, P. D. Simonson, F. Ye, I. Golding, T. Ng, W. Lopes, and P. R. Selvin, *Nano Lett.* **11**, 4074 (2011).
- Y. Wang, X. Li, X. Zhao, L. Xiao, H. Zeng, and H. Sun, *Nano Lett.* **16**, 448 (2016).
- N. S. Makarov, P. C. Lau, C. Olson, K. A. Velizhanin, K. M. Solntsev, K. Kieu, S. Kilina, S. Tretiak, R. A. Norwood, N. Peyghambarian, and J. W. Perry, *ACS Nano* **8**, 12572 (2014).
- C. Xu and W. W. Webb, *J. Opt. Soc. Am. B* **13**, 481 (1996).
- C. F. Zhang, F. Zhang, A. Cheng, B. Kimball, A. Y. Wang, and J. Xu, *Appl. Phys. Lett.* **95**, 183109 (2009).
- F. Todescato, I. Fortunati, S. Gardin, E. Garbin, E. Collini, R. Bozio, J. J. Jasieniak, G. Della Giustina, G. Brusatin, S. Toffanin, and R. Signorini, *Adv. Funct. Mater.* **22**, 337 (2012).
- M. D. Wissert, B. Rudat, U. Lemmer, and H. J. Eisler, *Phys. Rev. B* **83**, 113304 (2011).
- K. T. Early and D. J. Nesbitt, *Nano Lett.* **15**, 7781 (2015).
- A. M. van Oijen, R. Verberk, Y. Durand, J. Schmidt, J. N. J. van Lingen, A. A. Bol, and A. Meijerink, *Appl. Phys. Lett.* **79**, 830 (2001).
- A. Kojima, K. Teshima, Y. Shirai, and T. Miyasaka, *J. Am. Chem. Soc.* **131**, 6050 (2009).
- Z. K. Tan, R. S. Moghaddam, M. L. Lai, P. Docampo, R. Higler, F. Deschler, M. Price, A. Sadhanala, L. M. Pazos, D. Credgington, F. Hanusch, T. Bein, H. J. Snaith, and R. H. Friend, *Nat. Nanotechnol.* **9**, 687 (2014).
- J. Wang, N. Wang, Y. Jin, J. Si, Z. K. Tan, H. Du, L. Cheng, X. Dai, S. Bai, H. He, Z. Ye, M. L. Lai, R. H. Friend, and W. Huang, *Adv. Mater.* **27**, 2311 (2015).
- L. Dou, Y. M. Yang, J. You, Z. Hong, W. H. Chang, G. Li, and Y. Yang, *Nat. Commun.* **5**, 5404 (2014).
- G. Xing, N. Mathews, S. S. Lim, N. Yantara, X. Liu, D. Sabba, M. Gratzel, S. Mhaisalkar, and T. C. Sum, *Nat. Mater.* **13**, 476 (2014).
- F. Zhang, H. Zhong, C. Chen, X. G. Wu, X. Hu, H. Huang, J. Han, B. Zou, and Y. Dong, *ACS Nano* **9**, 4533 (2015).
- L. Protesescu, S. Yakunin, M. I. Bodnarchuk, F. Krieg, R. Caputo, C. H. Hendon, R. X. Yang, A. Walsh, and M. V. Kovalenko, *Nano Lett.* **15**, 3692 (2015).
- Y. Tian, A. Merdasa, M. Peter, M. Abdellah, K. Zheng, C. S. Ponseca, Jr., T. Pullerits, A. Yartsev, V. Sundstrom, and I. G. Scheblykin, *Nano Lett.* **15**, 1603 (2015).
- Y. S. Park, S. Guo, N. S. Makarov, and V. I. Klimov, *ACS Nano* **9**, 10386 (2015).
- F. Hu, C. Yin, H. Zhang, C. Sun, W. W. Yu, C. Zhang, X. Wang, Y. Zhang, and M. Xiao, *Nano Lett.* **16**, 6425 (2016).
- F. Hu, H. Zhang, C. Sun, C. Yin, B. Lv, C. Zhang, W. W. Yu, X. Wang, Y. Zhang, and M. Xiao, *ACS Nano* **9**, 12410 (2015).
- H. Utzat, W. Sun, A. E. K. Kaplan, F. Krieg, M. Ginterseder, B. Spokoyny, N. D. Klein, K. E. Shulenberger, C. F. Perkinson, M. V. Kovalenko, and M. G. Bawendi, *Science* **363**, 1068 (2019).
- M. A. Becker, R. Vaxenburg, G. Nedelcu, P. C. Sercel, A. Shabaev, M. J. Mehl, J. G. Michopoulos, S. G. Lambrakos, N. Bernstein, J. L. Lyons, T. Stoferle, R. F. Mahrt, M. V. Kovalenko, D. J. Norris, G. Raino, and A. L. Efros, *Nature* **553**, 189 (2018).
- C. Yin, L. Chen, N. Song, Y. Lv, F. Hu, C. Sun, W. W. Yu, C. Zhang, X. Wang, Y. Zhang, and M. Xiao, *Phys. Rev. Lett.* **119**, 026401 (2017).
- P. Tamarat, M. I. Bodnarchuk, J. B. Trebbia, R. Erni, M. V. Kovalenko, J. Even, and B. Lounis, *Nat. Mater.* **18**, 717 (2019).
- Y. Lv, C. Yin, C. Zhang, W. W. Yu, X. Wang, Y. Zhang, and M. Xiao, *Nano Lett.* **19**, 4442 (2019).
- D. Huber, M. Reindl, S. F. C. da Silva, C. Schimpf, J. Martín-Sánchez, H. Huang, G. Piredda, J. Edlinger, A. Rastelli, and R. Trotta, *Phys. Rev. Lett.* **121**, 033902 (2018).
- J. Chen, K. Zidek, P. Chabera, D. Liu, P. Cheng, L. Nuuttilla, M. J. Al-Marri, H. Lehtivuori, M. E. Messing, K. Han, K. Zheng, and T. Pullerits, *J. Phys. Chem. Lett.* **8**, 2316 (2017).
- W. Chen, S. Bhaumik, S. A. Veldhuis, G. Xing, Q. Xu, M. Gratzel, S. Mhaisalkar, N. Mathews, and T. C. Sum, *Nat. Commun.* **8**, 15198 (2017).
- G. Nagamine, J. O. Rocha, L. G. Bonato, A. F. Nogueira, Z. Zaharieva, A. A. R. Watt, C. H. de Brito Cruz, and L. A. Padilha, *J. Phys. Chem. Lett.* **9**, 3478 (2018).
- A. Pramanik, K. Gates, Y. Gao, S. Begum, and P. C. Ray, *J. Phys. Chem. C* **123**, 5150 (2019).
- Z. P. Hu, Z. Z. Liu, Y. Bian, S. Q. Li, X. S. Tang, J. Du, Z. G. Zang, M. Zhou, W. Hu, Y. X. Tian, and Y. X. Leng, *Adv. Opt. Mater.* **6**, 1700997 (2018).
- N. S. Makarov, S. Guo, O. Isaienko, W. Liu, I. Robel, and V. I. Klimov, *Nano Lett.* **16**, 2349 (2016).
- T. C. He, J. Z. Li, C. Ren, S. Y. Xiao, Y. W. Li, R. Chen, and X. D. Lin, *Appl. Phys. Lett.* **111**, 211105 (2017).
- Q. J. Han, W. Z. Wu, W. L. Liu, Q. X. Yang, and Y. Q. Yang, *Opt. Mater.* **75**, 880 (2018).
- Y. Xu, Q. Chen, C. Zhang, R. Wang, H. Wu, X. Zhang, G. Xing, W. W. Yu, X. Wang, Y. Zhang, and M. Xiao, *J. Am. Chem. Soc.* **138**, 3761 (2016).
- S. C. Pu, M. J. Yang, C. C. Hsu, C. W. Lai, C. C. Hsieh, S. H. Lin, Y. M. Cheng, and P. T. Chou, *Small* **2**, 1308 (2006).
- C. Becker, S. Burger, C. Barth, P. Manley, K. Jäger, D. Eisenhauer, G. Köppel, P. Chabera, J. Chen, K. Zheng, and T. Pullerits, *ACS Photonics* **5**, 4668 (2018).